



# APPLYING ARTIFICIAL INTELLIGENCE TO DETECT RETINAL DISEASES

Haitam Ettazi <sup>1</sup>  
Najat Rafalia  
Jaafar Abouchabaka

Received 31.05.2022.  
Accepted 21.09.2022.  
UDC – 005.934.2

Keywords:

*Convolutional neural network; Optical coherence Tomography; Transfer learning; Medical imaging; Image classification*

ABSTRACT

*Vision and eye health are one of the most crucial things in human life, it needs to be preserved to maintain the life of the individuals. Eye diseases such as CNV, DRUSEN, AMD, and DME are mainly caused due to the damages of the retina, and since the retina is damaged and discovered at late stages, there is almost no chance to reverse vision and cure it, which means that the patient will lose the power of vision partially and maybe entirely. Optical Coherence Tomography is an advanced scanning device that can perform non-invasive cross-sectional imaging of internal structures in biological tissues by measuring their optical reflections. This will help the ophthalmologists to take a clear look on the back of the eye and determine at early stages the damage caused to the retina, macula, and optic nerve. The aim of this study is to propose a novel classification model based on deep learning and transfer learning to automatically classify the different retinal diseases using retinal images obtained from Optical Coherence Tomography (OCT) device. We propose a deep CNN architecture and compared the obtained results with pre-trained models such as Inception V3 and VGG-16, our proposed CNN architecture gave an accuracy of 98.96% and Inception V3 model gave accuracy up to 99.27% on the test set.*



© 2023 Published by Faculty of Engineering

## 1. INTRODUCTION

OCT stands for Optical Coherence Tomography is an advanced scanning device that can perform non-invasive cross-sectional imaging of internal structures in biological tissues by measuring their optical reflections. According to Goldberg (2018). This will help the ophthalmologists to take a clear look on the back of the eye and determine at early stages the damage caused to the retina, macula, and optic nerve. Diagnosing or predicting these pathologies at early stages can increase the chance of curing the patients and restore vision

ability, it has been also proved that eye diseases don't just affect the retina and the patient's vision, but it has also a relation between heart diseases and hypertension, which means that predicting and diagnosing eye diseases at early stages can also save the health of the patient's heart.

Four main types of eye diseases are treated in this study:

**DME** Diabetic Macular Edema is a type of eye disease due to the damage of blood vessels in the retina. When left untreated, DME will cause the build-up of liquid in

<sup>1</sup> Corresponding author: Haitam Ettazi  
Email: [haitam.ettazi@uit.ac.ma](mailto:haitam.ettazi@uit.ac.ma)

the macula further leading to a swollen area on the retinal layer and consequently irreversible eye blindness.

**AMD** Age-related Macular Degeneration is damage affects the macula (small area at the center of the retina), leads to center-blind, and it is a blinding disease with no cure at present. This disease does not just affect the vision of the patient, but it can also cause heart diseases and hypertension, according to Al Qassimi et al (2022). The number of people living with macular degeneration is expected to reach 196 million worldwide by 2020 and increase to 288 million by 2040 according to INSERM.

**DRUSEN** One of the first signs of AMD pathology are called DRUSEN. Drusen are yellow deposits under the retina, they are not symptoms of eye diseases, but the appearance of a large number of them can lead to AMD and vision loss. According to Fraccaro et al (2015) ophthalmologists these days use OCT imaging scanning to detect DRUSEN and define their types if they are serious and can lead to AMD, or if they can disappear in Simonyan et al (2015), which gives them the opportunity to make prior decisions.

**CNV** Choroidal neovascularization is a very common vision-threatening disease that leads to vision loss. It involves the growth of new blood vessels that originate from the choroid through a break in the Bruch membrane into the sub-retinal pigment epithelium or sub-retinal space. According to Curcio et al (2018) and Banerjee et al (2015) any damage to the Bruch membrane can be complicated by CNV.

## 2. RELATED WORKS

Machine learning is nowadays used in different fields of medical imaging, computer-aided diagnosis in Natekin et al (2013), image segmentation in Anantrasirichai et al (2013) and image-guided therapy; this means that there are multiple areas in medicine, where machine learning methods can be applied to improve patients' health care. Different studies have been proposed to classify OCT images. Hussain et al (2018) proposed a classification model based on random forest classifier, with 15-fold cross-validation tests, to detect (AMD) or Diabetic Macular Edema (DME) using retinal features from Spectral Domain Optical Coherence Tomography (SD-OCT) images. The dataset contained 251 (59 normal, 177 AMD and 15 DME) images, and obtained the accuracy of 95 % while testing and 96 % in train set.

Lee et al (2019) proposed architecture to detect AMD diseases using Random Forest with a maximum of 100 trees is used for the classifier. The method achieved an AUC of 0.984 with a dataset of 384 (269 AMD, 115 control) OCT volumes. Lee et al (2019) have proposed a very deep CNN network architecture contained 9 CONV blocks and 2 FC layers. 2 max-pooling layers were placed after the 3rd and the 6th CONV blocks,

respectively. 1 global pooling layer was placed after the 9th CONV block. The spatial support of the filter in each of the CONV layers was set as 3 x 3 pixels. The number of the filters in the first three Conv layers was set to 32. In order to compensate for the information loss caused by max pooling, the number of filters in 2nd three CONV layers and 3rd three CONV layers were set to 64 and 128, respectively. Two FC layers followed the global pooling layer. The first FC layer included 512 neurons and the second one included 5 neurons. One dropout was set between these two FC layers with a dropout ratio of 0.5 to further avoid over-fitting. A softmax layer was placed at the end of the classifier.

The experiments on 269 OCT images showed that the average prediction accuracy of the CNN-based method was 0.866. The test set accuracy wasn't mentioned in their paper, we believe that such very deep architecture on a few data (269 images) can lead to over-fitting. One trick could have been done is to use data augmentation to get more data for training. Awais et al (2017) have worked on the classification of SD-OCT images using VGG-16 pre-trained model, to detect DME diseases on a dataset consisting of 32 OCT volumes (16 DME and 16 normal cases). Each volume contains 128 Bscans with resolution of 1,024px 512px. They did many experiments on the dataset combining CNN with other classifiers (KNN and Decision trees). The best configuration was obtained 93.5 %. One of their configurations gave 100% accuracy, by setting the  $k = 1$  in KNN classifier, and 2 FCL1, hence this leads also to over-fitting cause of the bad choice of parameters. Lee et al (2017) published a paper on classifying AMD diseases using a modified version of the VGG16 convolutional neural network on a total of 80,839 images (41,074 from AMD, 39,765 from normal) were used for training and 20,163 images (11,616 from AMD, 8,547 from normal) were used for validation. The training was then performed using multiple iterations each with a batch size of 100 images with a starting learning rate of 0.001 with stochastic gradient descent optimization. At each iteration, the loss of the model was recorded, and at every 500 iterations, the performance of the neural network was assessed using cross-validation with the validation set. The training was stopped when the loss of the model decreased and the accuracy of the validation set decreased. Accuracy in the area under the ROC curve (AUROC) was 92.77 %.

This is a very interesting paper indeed, due to the use of pre-trained model and regularization techniques to speed the learning phase and avoid over-fitting.

Another paper on classifying OCT images using deep learning methods by Mehta et al. (2018) for multi-label multiclass classification for OCT retinal images to diagnose patients who may exhibit multiple pathologies, the dataset consists of 36,150 images, applied data augmentation and modified version of Inception Resnet

V2 pre-trained model by removing the output activation layer softmax and replaced it with sigmoid. The goal of their study was to compare transfer learning with CNN from scratch the resulted work is accurate and exact match for transfer learning was 74.5% and 30.14% compared to 85.23% and 64.3% for direct learning. A paper was published recently that used the dataset that we are using in this study published by Nugroho et al (2019) comparison of Handcrafted and Deep Neural Network Feature Extraction for Classifying Optical Coherence Tomography (OCT) Images the deep neural network-based methods outperformed the handcrafted feature with 88% and 89% accuracy for DenseNet and ResNet compared to 50% and 42% for HOG and LBP respectively. The issue with this study is that they have split the dataset into 50% for training and 50% for validation. In this study, we are proposing different split of the data and different approaches.

### 3. PROPOSED APPROACH

**Machine learning approaches:** We have trained three classic machine learning classification algorithms, and we compared the results obtained of each algorithm based on the accuracy and training time.

**Decision trees classifier:** Decision trees classifier is one of the most popular machine learning algorithms used all along, we used Sklearn python library to fit decision tree classifier, after 38 minutes of training using Google Colabs GPU we obtained these results Table 1.

**Table 1.** Decision Tree Classifier Results

| Accuracy | Precision | Recall | F1-score |
|----------|-----------|--------|----------|
| 33,50%   | 33,25%    | 33,50% | 32,87%   |

**XGBOOST classifier:** After splitting our dataset and resized the images to have a shape of (224 by 224) pixels and converting the images to matrix data, we used Sklearn library to fit XGBOOST classifier to the training data. After 40 minutes of training we obtained the following results Table 2.

**Table 2.** XGBOOST Classifier Results

| Accuracy | Precision | Recall | F1-score |
|----------|-----------|--------|----------|
| 52,06%   | 51,91%    | 52,06% | 51,12%   |

**SVM Classifier:** We used the sklearn library to adapt the SVM classifier to the training data. After 13 minutes of training, the following results were obtained Table 3.

**Table 3.** SVM Classifier Results

| Accuracy | Precision | Recall | F1-score |
|----------|-----------|--------|----------|
| 40,20%   | 44,31%    | 40,20% | 40,29%   |

**Random Forest Classifier:** We used the sklearn library to adapt the SVM classifier to the training data. After 13 minutes of training, the following results were obtained Table4.

**Table4.** Random Forest Classifier Results

| Accuracy | Precision | Recall | F1-score |
|----------|-----------|--------|----------|
| 40,20%   | 44,31%    | 40,20% | 40,29%   |

**Deep learning approaches:** In this section we will demonstrate how we applied deep learning to classify and identify the retinal diseases, we focused on the use of convolution neural networks because they shows a good performance when dealing with images, we done many experiments, we changed the hyper-parameters and evaluated the obtained results. We also establish the use of some pre-trained models by tuning them to fit our dataset outputs.

**First CNN architecture:** the first CNN experiment architecture is composed of 3 Convolution layers and 3 Max pooling layers and one dense layer.

We obtained from this experiment an accuracy of **96, 97%** in validation set and **97, 52%** when testing on our test set data.

**Second CNN architecture:** We added to the first CNN architecture one dropout layer and one Batch normalization layers.

We obtained from this experiment an accuracy of **97, 20%** in validation set and **98, 96%** when testing on our test set data.

#### 3.1 Architecture interpretation

The model is sequential which allows us to create the model layer-by-layer. The architecture consists of convolutional layers, max- pooling layers, dropout layers, and fully connected layers.

The first layer is a convolutional layer with 32 filters each of size 3 x 3. We are also required to specify the input shape in the first layer, which is 224 x 224 x 3 in our case.

We will be using the Rectified linear unit (**ReLU**) activation function for all the layers except the final output layer. ReLU is the most common choice for activation function in the hidden layers and has shown to work pretty well

The second layer is a pooling layer. The pooling layers are used to reduce the dimension. Max Pooling with a 4x4 window only considers the maximum value in the 4x4 window. A dropout layer with dropout rate of 0.1 means 10% of the neurons will be turned off randomly as demonstrated by Simonyan et al (2015).

This helps prevent over-fitting by making all the neurons learn something about the data and not rely on just a few neurons. Randomly dropping neurons during training means other neurons will have to do the work of the turned-off neurons, thus generalizing better and

prevent over-fitting The third layer is again a convolutional layer of 512 filters each of size 3 x 3 followed by another max-pooling layer of 3x3 window. Usually, the number of filters in the convolutional layer grows after each layer. The first layers with a lower number of filters learn simple features of the images whereas the deeper layers are again convolutional layers with 32 filter size followed by a Batch normalization layer. We need to flatten the 3D feature map output

from the convolutional layer to 1D feature vectors before adding in the fully connected layers. This is where the flattening layer comes in. The following dense layer (fully connected layer) has 128 neurons. The final output layer is another dense layer that has a number of neurons equal to the number of classes. The activation function is softmax because it is a multi-class classification problem (figure 1).

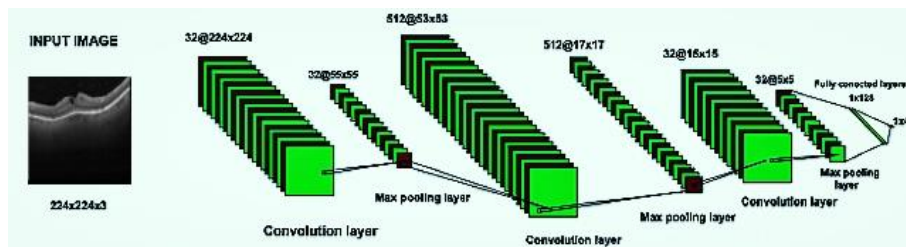


Figure1. Our proposed CNN architecture

**Inception V3 Model:** We used Inception V3 pre-trained weights to classify our images; we removed the first three top layers and changing the output layer to have four neurons corresponding to our number of classes (Figure 2).

**VGG-16 Model:** We used VGG-16 as proposed by Deng et al (2009) pre-trained weights to classify our images same as we did with Inception V3 model, we removed the first three top layers and changing the output layer to have four neurons corresponding to our number of classes (figure 3).

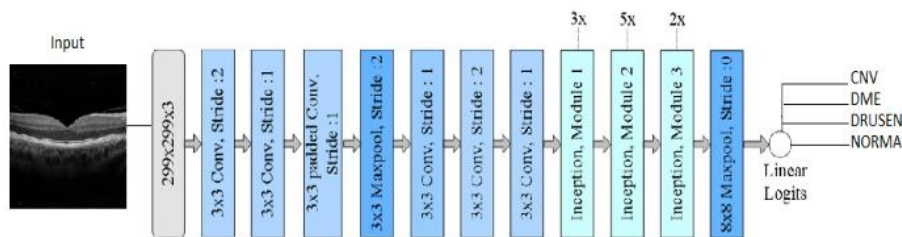


Figure 2. InceptionV3 Adapted Mode



Figure 3. VGG-16 Architecture Adapted version

**ResNET50 Model:** We used ResNET50 pre-trained weights to classify our images same as we did with InceptionV3 and VGG16 models, we removed the first

three top layers and changing the output layer to have four neurons corresponding to our number of classes (figure 4).

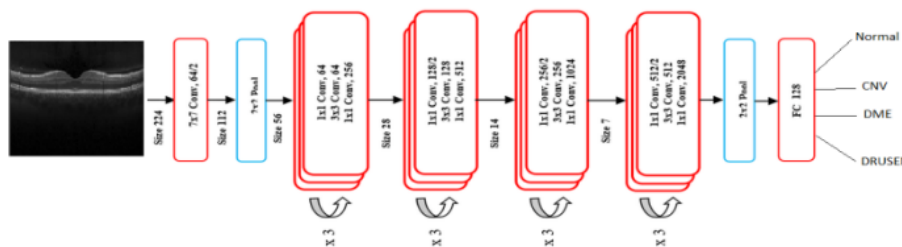


Figure 4. ResNET50 Architecture Adapted Mode

### 3.2 Compiling and training the models

All the models are compiled with categorical cross-entropy loss function and the Adam as an optimization algorithm, except the InceptionV3 model where we tried both Adam and rmsprop. The last one gave better results. The accuracy metric is used to evaluate the model. Training the model using a GPU speed up the training process, we set the number of epochs to 15 and use a regularization method Early Stopping as suggested in Deng et al (2009), in our study, we tell Early Stopping to monitor validation-accuracy and if it does not improve for 10 epochs continuously, stop the training process. The model checkpoint is used to save the model.

The monitor parameter allows us to set a metric that we want to keep an eye on. In our case, we only save the model when the validation accuracy is the max. We save the best model to be used later to make predictions and thus evaluate the models' performance.

### 3.3 Dataset overview and preprocessing

In this paper, the dataset used is the OCT images from Srinivasan et al (2014); this dataset is grouped into 3 folders (train, test, val). This dataset contains subfolders for each image category (NORMAL, CNV, DME and DRUSEN). There are 84495 images (JPEG) and 4 categories (NORMAL, CNV, DME and DRUSEN).

Our dataset was taken from different research labs, what makes the sizes of the images varies (496, 768, 3), (496, 1024, 3), (496, 512, 3), (496, 1536, 3), (512, 512, 3) the first two values refers to the width and height of the image, and the third one refers to the image channels, meaning in this case that the images are in RGB (Table 5, Table 6).

Table 5. DATASET original split

|               | Training     | Testing    | Validation |              |
|---------------|--------------|------------|------------|--------------|
| <b>CNV</b>    | 37205        | 242        | 8          | <b>37455</b> |
| <b>DME</b>    | 11348        | 242        | 8          | <b>11598</b> |
| <b>DRUSEN</b> | 8616         | 242        | 8          | <b>8866</b>  |
| <b>NORMAL</b> | 26315        | 242        | 8          | <b>26565</b> |
|               | <b>83484</b> | <b>968</b> | <b>32</b>  | <b>84484</b> |

Table 6. DATASET Distribution after resampling

|               | Training     | Testing    | Validation   |              |
|---------------|--------------|------------|--------------|--------------|
| <b>CNV</b>    | 33039        | 242        | 4174         | <b>37455</b> |
| <b>DME</b>    | 7182         | 242        | 4174         | <b>11598</b> |
| <b>DRUSEN</b> | 4450         | 242        | 4174         | <b>8866</b>  |
| <b>NORMAL</b> | 22149        | 242        | 4174         | <b>26565</b> |
|               | <b>66820</b> | <b>968</b> | <b>16696</b> | <b>84484</b> |

**Data Rescaling:** Importing the images with the original sizes will lead to use big part of hardware resources and the time of processing the images will highly increase, we reduced the image sizes to 224 X 224 pixels, same as Imagenet as proposed by Shafiq et al (2022) in order to apply experiment on pre-trained models.

**Data Resampling:** The dataset is splitted into 3 folders as explained in the previous section, with only 8 images per class for validation and 242 images for test and the rest for training as detailed in Table 6, this split is not efficient and can lead to extreme over-fitting. We made another split of 80% for training, 20% for validation (Table 6) and after constructing our model we tested our model on 968 images.

## 4. RESULTS AND DISCUSSION

After compiling our first CNN architecture we obtained an accuracy of **96,97%** in validation set and **97,52%** when testing on our test set data (figure 5, figure 6).

After the second experiment of our CNN architecture (after adding the regularization terms) we obtained accuracy up to **97,29%** and accuracy of **98,96%** while testing. Meaning when we added the two regularization terms the accuracy did enhance for both validation and testing.

The training time of the VGG16 model was 16 minutes per epoch, we obtained an accuracy of **94,75%** on validation and in testing the model. The accuracy in the validation part didn't improve the 10 first epochs until early stopping algorithm stopped the training process.

Our experiment on the ResNET50 model, the training time was 20 minutes per epoch, we obtained an accuracy of **95,57%** on validation and in testing the model.

We obtained an accuracy up to **99.03%** in training and **100%** in the validation part, and accuracy of **99.27%** in 986 testing images. This experiment outperformed all the other results.

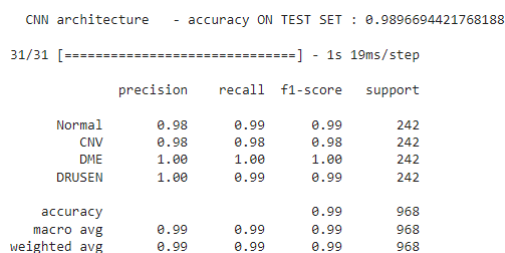


Figure 5. Precision and Recall of each class obtained by second CNN architecture

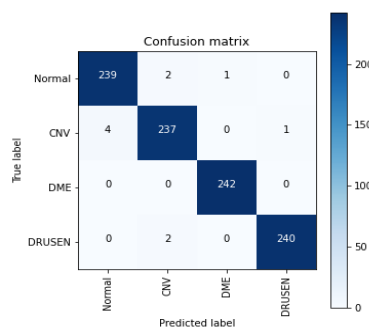


Figure 6. Confusion matrix obtained by the second CNN architecture

Predictive labels on the X-axes and true labels on the Y-axes, we have used 968 images to test our model, the blue cells shows the correct predicted images meaning the predicted labels matches the actual labels of the images, in this case the model correctly predicted 958 images out of 968 images where the DME images were 100% correctly predicted and the Wight cells show the incorrectly predicted labels which 10 in this case (figure 7).

Inception V3- Rmsprop optimizer - accuracy ON TEST SET : 0.9927685950413223

|        | precision | recall | f1-score | support |
|--------|-----------|--------|----------|---------|
| Normal | 1.00      | 0.98   | 0.99     | 242     |
| CNV    | 0.98      | 1.00   | 0.99     | 242     |
| DME    | 1.00      | 1.00   | 1.00     | 242     |
| DRUSEN | 1.00      | 0.99   | 0.99     | 242     |

Figure 7. Model’s accuracy obtained by the Inception model while testing

The performance on the test data is consistent with the performance on the training data. DME, DRUSEN and Normal images have a great precision value of 100%, in all the evaluation metrics. CNV have lower precision value compared to other classes (figure 8).

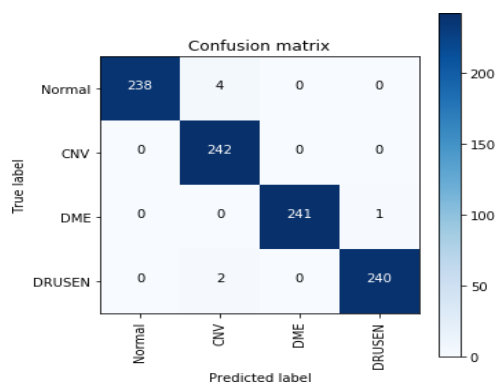


Figure 8. Model’s accuracy obtained by the Inception model while testing

This model was able to correctly predict 961 out of 968 images, meaning only 7 images were incorrectly classified, this shows better results compared to the previous confusion matrix where the 2nd CNN models miss-classified 13 images. The CNV category is better classed here compared to the previous confusion matrix

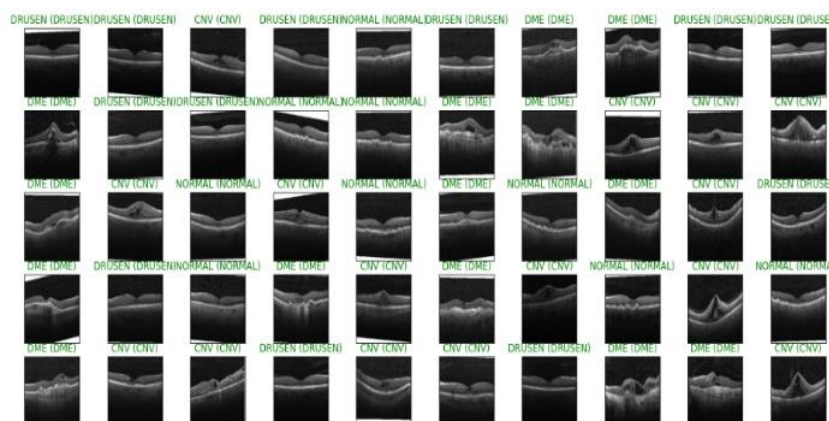


Figure 11. Comparisons between experts and our model

of the 2nd CNN architecture, and the test accuracy improved as well, all the instances of CNV class were correctly classified (figure 9, figure 10).

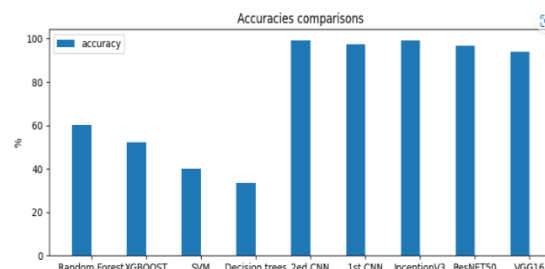


Figure 9. Comparisons of the results obtained by our experiments

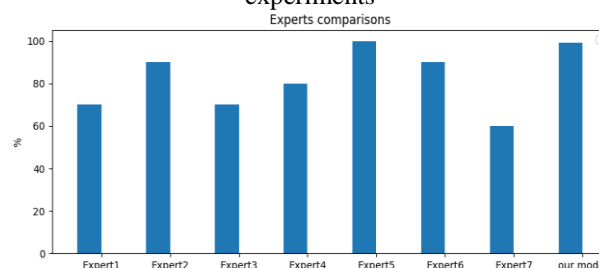


Figure 10. Comparisons between experts and our model

In order to evaluate our models and see if they give good results compared to OCT radiologists’ experts, we obtained diagnosis of 7 OCT radiologist, by asking them to label 10 images corresponding to the category. The experts were given the enough time to make their own decision on the images, from all doctors, only one of them accurately classified the 10 images. Another thing to notice is that all the doctors have correctly classified the DME and NORMAL images, and some of them struggle to diagnose images that contain CNV.

Our model outperformed the diagnosis of 6 out of 7 OCT experts in term of accuracy. It took the model only 3 seconds to predict the 10 images. Then we tested 50 images on our model, our model successfully classed all the images correctly as illustrated in figure 11.

## 5. CONCLUSION

This work represents case study and aims to develop and propose a new novel classification model based on deep learning to automatically detect and diagnose retinal images better than the diagnosis of experts in OCT radiology and also previous published papers.

To achieve research objectives we conducted many experiments using classic machine learning classification algorithms and deep convolutional neural nets methods. As turned out, our proposed CNN model outperformed all other classifiers and approaches, as well as the diagnosis of OCT experts. The results has shown that the use of Convolutional neural networks can give very interesting results in image classification and can be used to asses doctors in medical diagnose and opens up to a new, simple and effective method for early CNV, DME and DRUSEN detection. We have also seen that the use

of some pre-trained models can enhance the results in time and model effectiveness.

Our approaches shows good results in term of classification performance, yet we didn't trained our models for long epochs due to the hardware limitations, and we haven't test our models in different OCT dataset to see if they can perform as well as they did in this data.

As perspectives, we would study further many related problems and test our models in different datasets to diagnose more retinal diseases. We also aim to integrate our model directly into an OCT scanning device to assess the ophthalmologists in making decisions.

## References:

- Al Qassimi, N., Kozak, I., Al Karam, M., Neri, P., Aduriz-Lorenzo, P. M., ..., & Emirates Society of Ophthalmology. (2022). Management of Diabetic Macular Edema: Guidelines from the Emirates Society of Ophthalmology. *Ophthalmology and Therapy*, 11(5), 1937-1950. <https://doi.org/10.1007/s40123-022-00547-2>.
- Anantrasrichai, N., Achim, A.M., Morgan, J. E., Erchova, I., & Nicholson, L.B. (2013). SVM-based texture classification in Optical Coherence Tomography. 2013 IEEE 10th International Symposium on Biomedical Imaging, 1332-1335.
- Awais, M., Müller, H., Tang, T. B., & Mériaudeau, F. (2017). Classification of SD-OCT images using a Deep learning approach. In 2017 IEEE International Conference on Signal and Image Processing Applications (ICSIPA) (pp. 489-492).
- Banerjee, S., & Roy Chowdhury, A. (2015). Case Based Reasoning in the Detection of Retinal Abnormalities Using Decision Trees. *Procedia Computer Science*, 46, 402-408. <https://doi.org/10.1016/j.procs.2015.02.037>.
- CNIL. (n.d.). Apprentissage automatique. Retrieved from <https://www.cnil.fr/fr/definition/apprentissage-automatique>.
- Curcio C. A. (2018). Soft Drusen in Age-Related Macular Degeneration: Biology and Targeting Via the Oil Spill Strategies. *Investigative Ophthalmology & Visual science*, 59(4), AMD160-AMD181. <https://doi.org/10.1167/iovs.18-24882>.
- Deng, J., Dong, W., Socher, R., Li, L.-J., Li, K., & Li, F.-F. (2009). ImageNet: A Large-Scale Hierarchical Image Database. In IEEE Conference on Computer Vision and Pattern Recognition.
- Fraccaro, P., Nicolo, M., Bonetto, M., Giacomini, M., Weller, P., Traverso, C. E., Prosperi, M., & OSullivan, D. (2015). Combining macula clinical signs and patient characteristics for age-related macular degeneration diagnosis: a machine learning approach. *BMC ophthalmology*, 15, 10. <https://doi.org/10.1186/1471-2415-15-10>.
- Goldberg, J. (2018). 2018 Weston Lecture. Retrieved from Weston Eye Center website: [www.westoneyecenter.com/Glaucoma](http://www.westoneyecenter.com/Glaucoma).
- Hussain, M. A., Bhuiyan, A., D Luu, C., Theodore Smith, R., H Guymer, R., Ishikawa, H., S Schuman, J., & Ramamohanarao, K. (2018). Classification of healthy and diseased retina using SD-OCT imaging and Random Forest Algorithm. *PIOS ONE*, 13(6), e0198281. <https://doi.org/10.1371/journal.pone.0198281>.
- Inserm. (n.d.). Dégénérescence maculaire liée à l'âge (DMLA). Retrieved from <https://www.inserm.fr/dossier/degenerescence-maculaire-liee-age-dmla>.
- Lee, C., M. Baughman, D., & Lee, A. (2017). Deep Learning Is Effective for Classifying Normal versus Age-Related Macular Degeneration Optical Coherence Tomography Images. *Ophthalmology Retina*.
- Lee, J., Prabhu, D., Kolluru, C., Gharaibeh, Y., Zimin, V. N., Bezerra, H. G., & Wilson, D. L. (2019). Automated plaque characterization using deep learning on coronary intravascular optical coherence tomographic images. *Biomedical optics express*, 10(12), 6497-6515. <https://doi.org/10.1364/BOE.10.006497>.
- Mehta, P., Lee, A., Lee, C., Balazinska, M., & Rokem, A. (2018). bioRxiv 316349. Retrieved from <https://doi.org/10.1101/316349>.

- Natekin, A., & Knoll, A. (2013). Gradient boosting machines, a tutorial. *Frontiers in neurorobotics*, 7, 21. <https://doi.org/10.3389/fnbot.2013.00021>.
- Nugroho, K. A. (2019). Class Centroid Based Convolutional Neural Network for Skin Cancer Detection. In 2019 2nd International Conference on Bioinformatics, Biotechnology and Biomedical Engineering (BioMIC) - Bioinformatics and Biomedical Engineering (pp. 1-6).
- Shafiq, M., & Gu, Z. (2022). Deep Residual Learning for Image Recognition: A Survey. *Applied Sciences*, 12(18), 8972. <https://doi.org/10.3390/app12188972>.
- Simonyan, K., & Zisserman, A. (2015). *Very Deep Convolutional Networks for Large-Scale Image Recognition*. ICLR.
- Srinivasan, P. P., Kim, L. A., Mettu, P. S., Cousins, S. W., Comer, G. M., Izatt, J. A., & Farsiu, S. (2014). Fully automated detection of diabetic macular edema and dry age-related macular degeneration from optical coherence tomography images. *Biomedical optics express*, 5(10), 3568–3577. <https://doi.org/10.1364/BOE.5.003568>.

---

**Haitam Ettazi**

Faculty of Sciences, University Ibn  
Tofail,  
Kenitra  
Morocco  
[haitam.ettazi@uit.ac.ma](mailto:haitam.ettazi@uit.ac.ma)  
ORCID 0000-0002-7303-3044

**Najat Rafalia**

Faculty of Sciences, University Ibn  
Tofail,  
Kenitra  
Morocco  
[najar.rafallia@uit.ac.ma](mailto:najar.rafallia@uit.ac.ma)

**Jaafar Abouchabaka**

Faculty of Sciences, University Ibn  
Tofail,  
Kenitra  
Morocco  
[jaafar.abouchabaka@uit.ac.ma](mailto:jaafar.abouchabaka@uit.ac.ma)

---